© Universiti Tun Hussein Onn Malaysia Publisher's Office

IJIE

Journal homepage: http://penerbit.uthm.edu.my/ojs/index.php/ijie
ISSN : 2229-838X e-ISSN : 2600-7916

The International Journal of Integrated Engineering

Influence Coefficients for a Single Superficial Cracked Thick Cylinder Under Torsion and Bending Moments

O. M. Al-moayed[1*], A. K. Kareem[1,2], A. E. Ismail[1], S. Jamian[1], M. N. Nemah[3]

[1]Faculty of Mechanical and Manufacturing Engineering,
Universiti Tun Hussein Onn Malaysia, Batu Pahat, 86400, MALAYSIA

[2]Faculty of Air Conditioning and Refrigeration Techniques Engineering, Department,
Al-Mustaqbal University College, Babylon, IRAQ

[3]Engineering Technical College-Najaf,
Al-Furat Al-Awsat Technical University, Najaf, 32001, IRAQ

*Corresponding Author

DOI: https://doi.org/10.30880/ijie.2020.12.04.013
Received 12 January 2020; Accepted 21 April 2020; Available online 30 April 2020

Abstract: In this paper, finite element analysis software, ANSYS, is used to calculate mode I, mode II and mode III SIFs for a single semi-elliptical surface crack located on a thick cylinder. Two crack positions were examined, external and internal cracks investigated under remote bending and torsion loading, separately. The ratio of the crack depth to crack length ranging from 0.4 to 1.2, while the ratio of crack depth to cylinder wall thickness vary between 0.2, 0.5 and 0.8, and the ratio of the cylinder's internal radius to the cylinder's wall thickness is 4. It is found for both bending and torsion, SIFs distributed symmetrically along the crack front, and the crack aspect ratio strongly affect the location of the maximum value. Generally, external cracks showed slightly higher SIFs than that of internal cracks. For bending loading, the effect of relative crack depth is higher than to that of torsion loading for the same crack configurations. For mode III, internal cracks showed a resistance to crack growth, dissimilar to external crack.

Keywords: Semi-elliptical surface crack, thick cylinder, FEM, ANSYS, SIFs

1. Introduction

Cylindrical structures, for example, pressure vessels and hollow pipes, are among the commonly used mechanical component in the industry. Similar to any other component, these structures expected to fail after approaching its designed service life. Sometimes, these structures do not withstand until reaching the estimated life, and a premature failure occurs. Practically, many reasons can accelerate the collapse of the pipe, for instance, improper operating, manufacturing errors or defects, and the existence of cracks. Surface cracks act as a stress concentration role in the component; therefore, the stress state in the crack region is higher than elsewhere on the element. Due to this increment in stress, which may exceed material yielding and lead to failure or break.

Basically, the original or the initial shape of the crack is irregular, but the crack taking an approximate semi-elliptical shape after few cyclic loadings [1]. In order to describe the structural integrity of a cracked structure, the stress intensity factor (SIFs) must be known. In fracture mechanics field, SIFs considered a fundamental parameter which is used to assess the crucial state of a crack [2].

The evaluation of stress intensity factor took a great interest in the research field due to its importance for fatigue life estimation. Abundant studies conducted for cracked plates, solid and hollow cylinders. In [3] performed the first attempt to resolve the problem of a cracked cylinder, where an engineering estimation has been applied.

In [4] determined the SIFs of surface cracks in plates and cylinder, besides the effect of the residual stress along with geometry on SIFs distribution. Meanwhile, [5-6] numerically investigated the problem of a slanted edge crack in plates, where tension and bending loadings were deemed.

*Corresponding author: ammorey99@gmail.com

Another study [7] applied 3-D finite element analysis (FEA) to determine SIFs coefficients for a wide range of surface crack located on pipe and rod, a focus was on the surface and deepes[t points on the crack front. In [8] obtained the value of SIFs of a semi-elliptical crack in a solid pipe, where tension, torsion and combination of both loadings were considered. In other hand, [9-10] applied FEA to compute the SIFs of a single crack in round bar under bending, torsion and combination of both loadings.

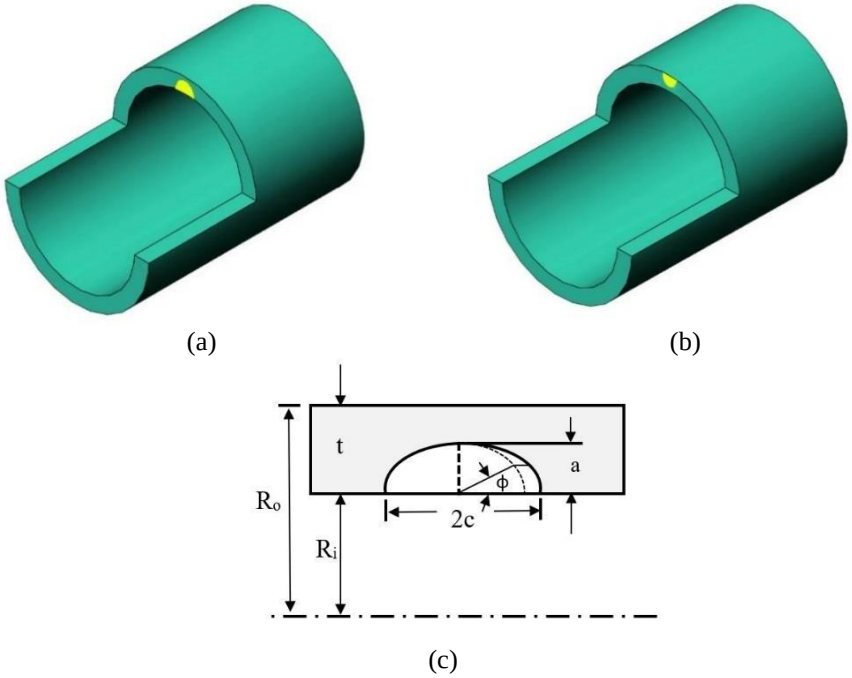

Fig. 1 - The problem outline (a) inner semi-elliptical crack; (b) outer semi-elliptical crack; (c) cross-sectional description of the crack geometry

Besides, [11] utilized 3-D finite element method to calculate the influence coefficients for mode I of a single longitudinal crack located internally and externally on thin and thick pressurized cylinders. 3-D FE has been performed in [12-13] to analyze the problem of hollow cylinder containing single edge crack subjected to bending and axial tension separately. In addition, [14-15] introduced composite theoretical and numerical method to evaluate SIFs of high aspect ratios of inner surface cracks in hollow cylinders.

Weight function method has been utilized in [16] to derive a closed form to determine SIFs at the deepest point on the crack front of a single circumferential interior crack in a thin cylinder, this study applicable to cracks with high aspect ratios. Whilst [17] solved mode II and mode III of externally cracked hollow cylinder problem under torsional loading by the use of FEM. While in [18] applied 3-D FEA to computed all the three modes of failure for a hollow cylinder with an external crack subjected to different types of loadings.

Recently, [19-20] performed a three-dimensional analysis to calculate SIFs for external and internal crack located on thin and thick cylinder exposed to internal pressure and tension loadings.

However, despite the available solutions in the literature, a hollow cylinder with an outer and inner semi-elliptical crack subjected to bending and torsion appears to be very scarce.

This study investigates all three modes of failure for a thick cracked hollow cylinder with a single external and internal crack. Bending and torsion loadings deemed, where each load applied separately through remote point. To involve an ample assortment of crack geometry, crack aspect ratio, *a/c*, (ratio of crack depth to half of crack length), vary from 0.4 to 1.2. While, relative crack depth, *a/t*, (ratio of crack depth to pipe wall thickness), changes between 0.2, 0.5 and 0.8. The finite element software, ANSYS utilized for each modelling and analysis procedures. The results presented in the form of normalized SIFs to provide more generalization.

2. Finite Element Modeling

This research, utilizes ANSYS, Finite element software [21], to model and analyze the cracked thick hollow cylinder, as shown in figure 1. A hollow cylinder with length, L, internal radius, R_i, external radius, R_o, and cylinder wall thickness, t, comprising single semi-elliptical crack of depth, a, and length of $2c$, placed on the inner and outer surfaces of the cylinder as shown in figure 2.

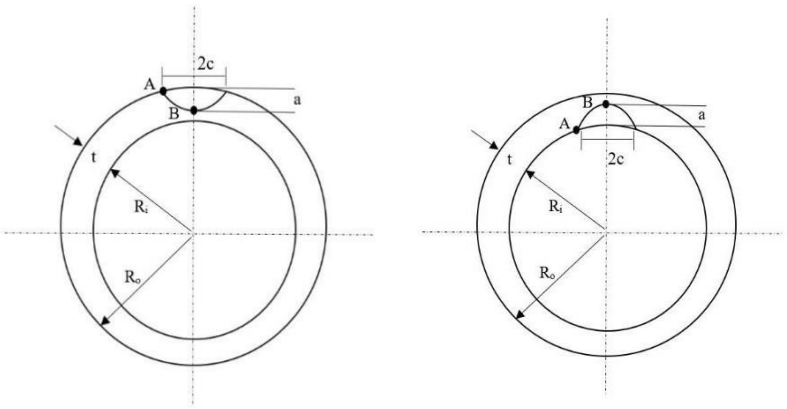

(a) **(b)**

Fig. 2 - Description of cylinder geometry with (a) external, and (b) internal peripheral semi-elliptical crack

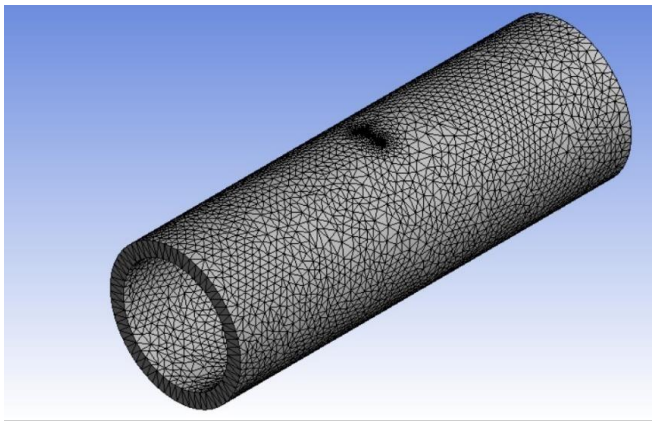

(a)

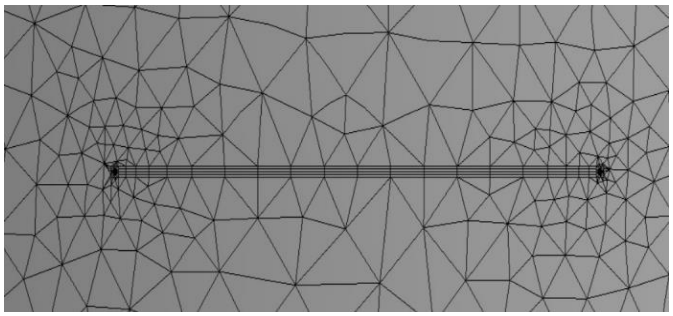

(b)

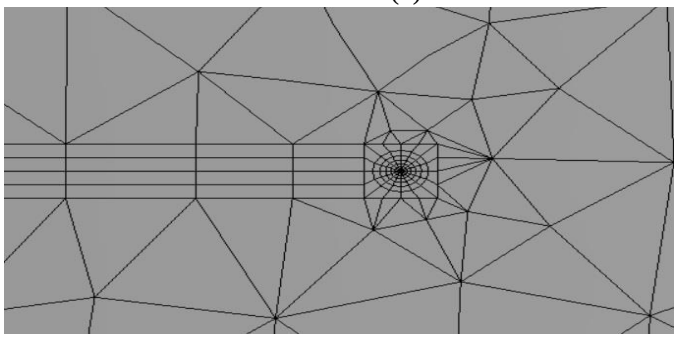

(c)

Fig. 3 - Detail of mesh where (a) the entire cylinder; (b) zone around the crack tip; (c) close-up to the crack tip

Commonly, in order to illustrate the geometry of the crack, two dimensionless parameters are required, they are, *a/c*, defining the crack shape, and, *a/t*, demonstrating the depth of the crack with respect to the cylinder wall thickness, which is also known as crack aspect ratio and relative depth of crack, respectively. Another dimensionless factor used to define the position on the crack front, which is called normalized crack front, $2\phi/\pi$, where ϕ, is the parametric angle of elliptical crack. The shape ratio for the crack assumed to change from 0.4 to 1.2, and for each value of shape ratio, three values of depth ratio vary between 0.2, 0.5 and 0.8. For all the considered cases in this study, R_i/R_o =0.8, and R_i/t =4, while the Poisson's ratio assumed to be 0.3, and Young's modulus is 200GPa.

The cylinder with the abovementioned parameters and properties modelled, which is the initial stage, the next step is to insert the crack and then mesh the overall model. For the mesh, due to the rapid changes in the region nearby the crack front, which is the area of interest, a very fine mesh-element used for this region, whilst a coarse mesh-element used for the remaining model as shown in Figure 3. In the final stage, the boundary conditions applied and postprocessing, then extract the results. For the all considered loading conditions, one of the cylinder ends is fixed, and the other end connected to a remote point, where the load applied through this point to the model. It is noteworthy that the applied load maintained in the elastic limits to avert large plastic deformations.

One of the built-in features in ANSYS is the capability to generate number of contours around the crack tips along the crack front, as shown in Figure 4, where SIFs for each contour is determined. The outmost contour with respect to the crack tip always provide more reliable results, and vice versa for the nearest one which gives unreliable results due to material shrinkage in this region [22]. For this study, six contours created, and since no difference between the 5th and 6th contour results, the result of the fifth contour was nominated.

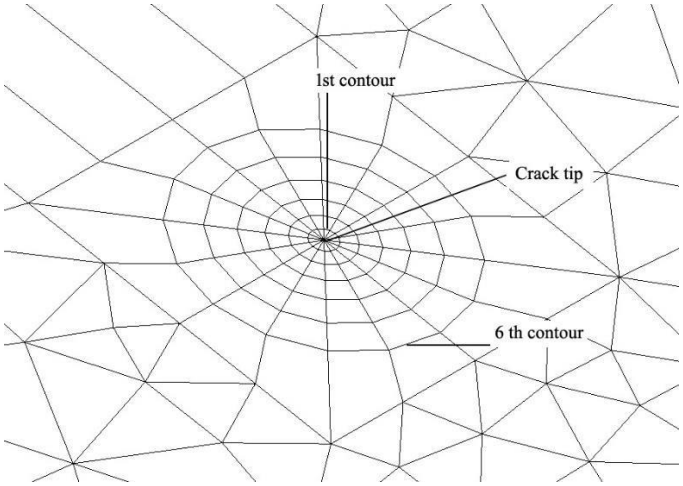

Fig. 4 - Orientation of generated contours around the crack tip

3. Evaluation of SIFs

The calculated values of SIFs that have been extracted from ANSYS were used to produce the SIF coefficients for bending and torsion, in term of mode I, mode II and mode III. For bending loading, the normalized SIF coefficient can be calculated as following [7] :

$$F_{I,B} = \frac{K_{I,cal}}{\sigma_b \sqrt{\pi a/Q}} \quad (1)$$

Where $F_{I,B}$ is the normalized mode I SIF coefficient under bending loading, $K_{I,cal}$ is the calculated mode I SIF by ANSYS under bending loading, σ_b, is the maximum bending stress, a, crack depth and Q, is the shape factor for an elliptical crack, which is determined by the subsequent formula [7] :

$$Q = 1 + 1.464\,(a/c)^{1.65} \quad \text{for a/c} \leq 1 \quad (2)$$

$$Q = 1 + 1.464\,(c/a)^{1.65} \quad \text{for a/c} > 1 \quad (3)$$

On the other hand, under unadulterated torsional loading conditions, mode I SIFs = 0 [17], therefore, only mode II and mode III are calculated and then normalized according to following [23]:

$$F_{II,T} = \frac{K_{II,cal}}{\tau_{max}\sqrt{\pi a/Q}} \quad (4)$$

$$F_{III,T} = \frac{K_{III,cal}}{\tau_{max}\sqrt{\pi a/Q}} \quad (5)$$

Where $F_{II,T}$ and $F_{III,T}$ are the normalized mode II and mode III SIFs coefficients under torsion loading respectively. While $K_{II,cal}$ and $K_{III,cal}$ denoting to the calculated values of stress intensity factors for mode II and III severally, and τ_{max}, is the maximum shear stress.

4. Result and Discussion

4.1 Model validation

Before proceeding the analysis procedure, a fundamental task is to investigate whether the proposed model for this study appropriates to perform the analysis. Furthermore, the capability of this model examined in term of accuracy with respect to those of the available models in the literature. To do so, the normalized SIFs coefficients of an axial crack, F_{axial}, exposed to internal pressure loading were compared to those of [11]. Figure 5 illustrates the comparison of both models for the same crack configurations, where the distribution of normalized SIFs plotted against the normalized crack front. Based on the results, it can be inferred that both models offering good agreement and the current suggested model is decent to carry out the analysis for the remaining crack configurations.

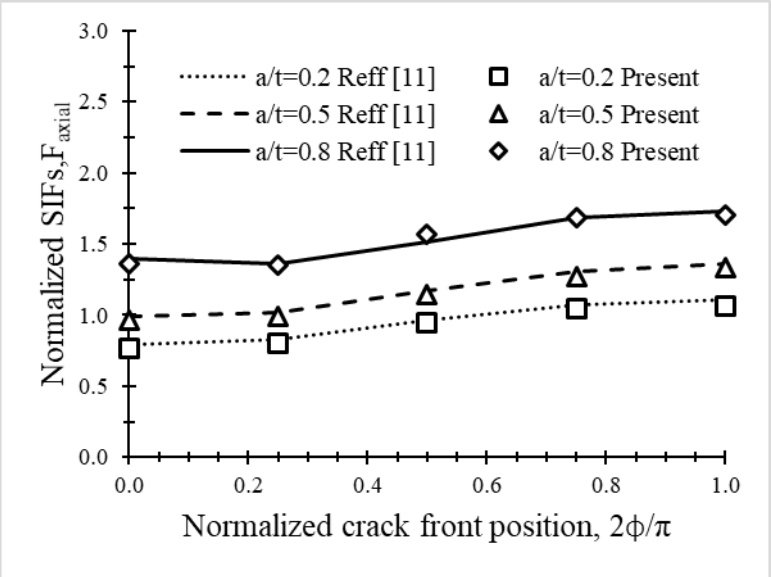

Fig. 5 - The validation of the proposed model with respect to [11]

4.2 SIFs coefficients under bending loading

A thick hollow cylinder with single surface crack, examined under bending moment loading applied remotely to the model. The crack positioned on the external and internal surface of the cylinder respectively. Five values of crack shape ratio, *a/c*, starting with 0.4 until 1.2 with 0.2 increments were tested to explore the effect of this ratio on the distribution of SIFs, while three values for the relative depth ratio, *a/t*, 0.2, 0.5 and 0.8 to check the impact of crack depth.

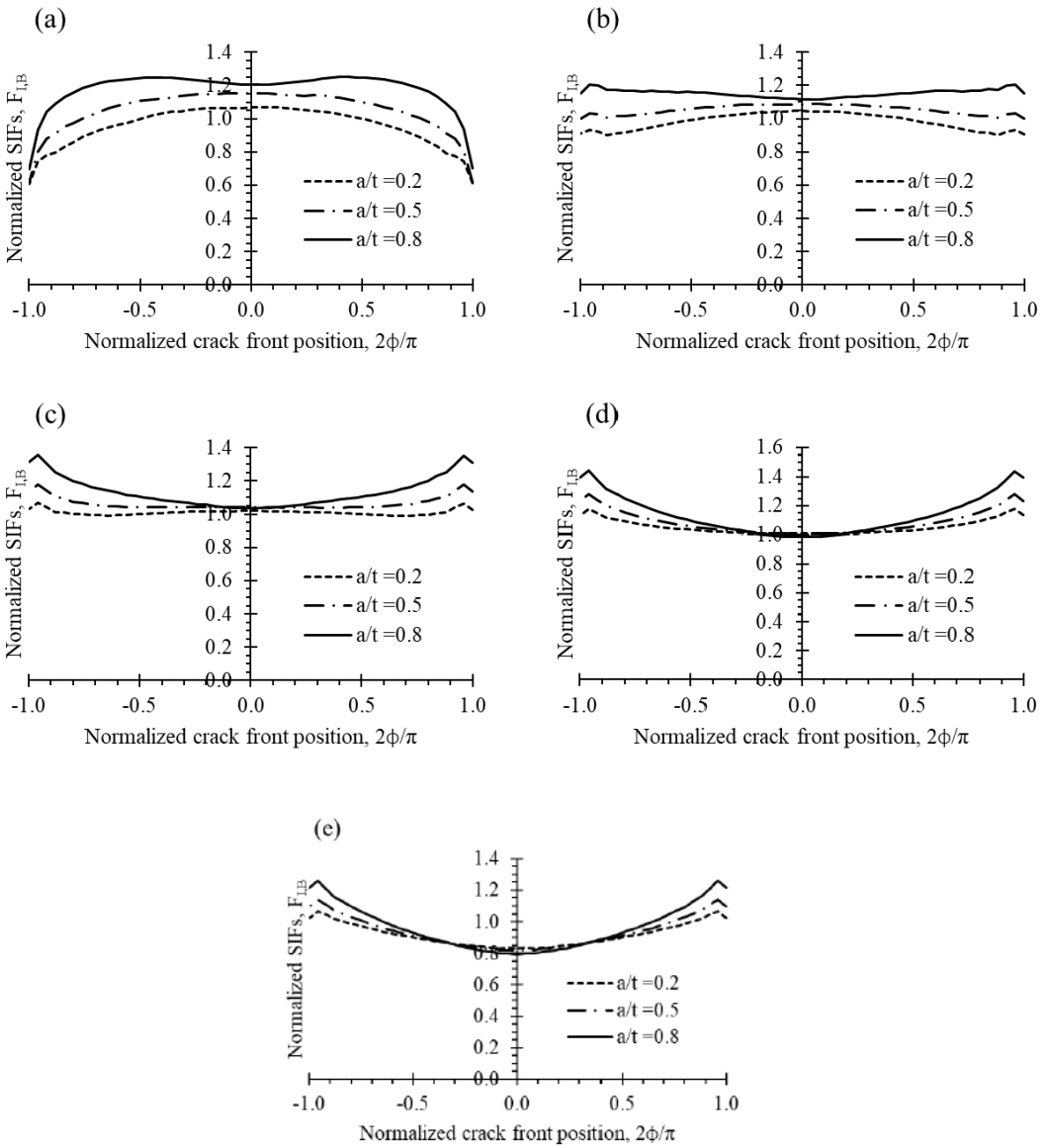

Fig. 6 - Distribution of mode I influence coefficients with respect to the crack front, for an external crack subjected to bending, where (a) a/c=0.4, (b) a/c=0.6, (c) a/c=0.8, (d) a/c=1, and (e) a/c=1.2

Figure 6 illustrates the allocation of the normalized mode I SIFs in term of normalized crack front position for an external surface crack, subjected to bending. It can be inferred that SIFs distribution is symmetric and the application of various aspect ratios, produces several curve profiles shapes. This is due to the change in the location where the maximum value of SIFs attained. This is a well-known phenomenon called as transition effect, where the location of the maximum value of SIF shifted from the deepest point (B) to the surface point (A) Figure 2, (0.0 and 1.0) in the graph, respectively. A same transition effect noticed for same crack configurations but with different types of loading in [19] and [20]. Furthermore, it can be deduced that for slender cracks under bending moment, the propagation occurs at point (B) rather than at point (A), whereas for other crack shapes, the propagation appears clearly at surface points instead of deep points of the crack front.

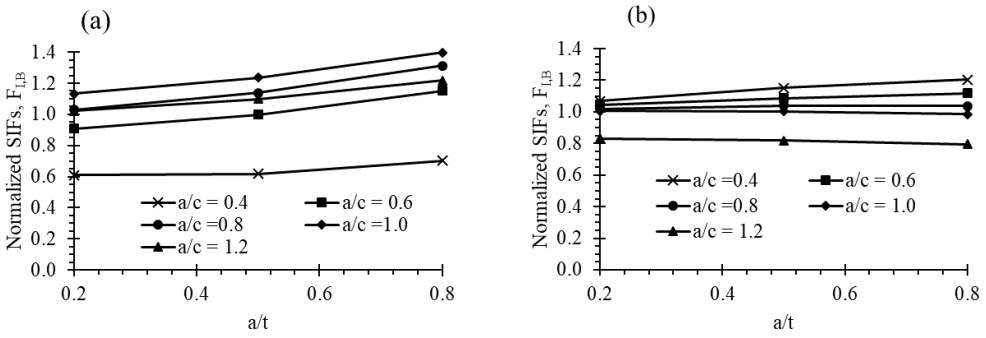

Fig. 7 - Behavior of SIFs in term of the relative depth of crack under bending at (a) surface point (A), (b) deepest point (B) on the front of an external crack

Figure 7 reveals the behavior of the surface point (A) and the deepest point (B) for an external crack with respect to the relative depth ratio of the crack in term of SIFs. At point (A), a direct proportion between shape ratio and SIFs, where any increase in the aspect ratio generates an increment in the SIFs, except for high aspect ratio, $a/c > 1$, which exhibited less values.

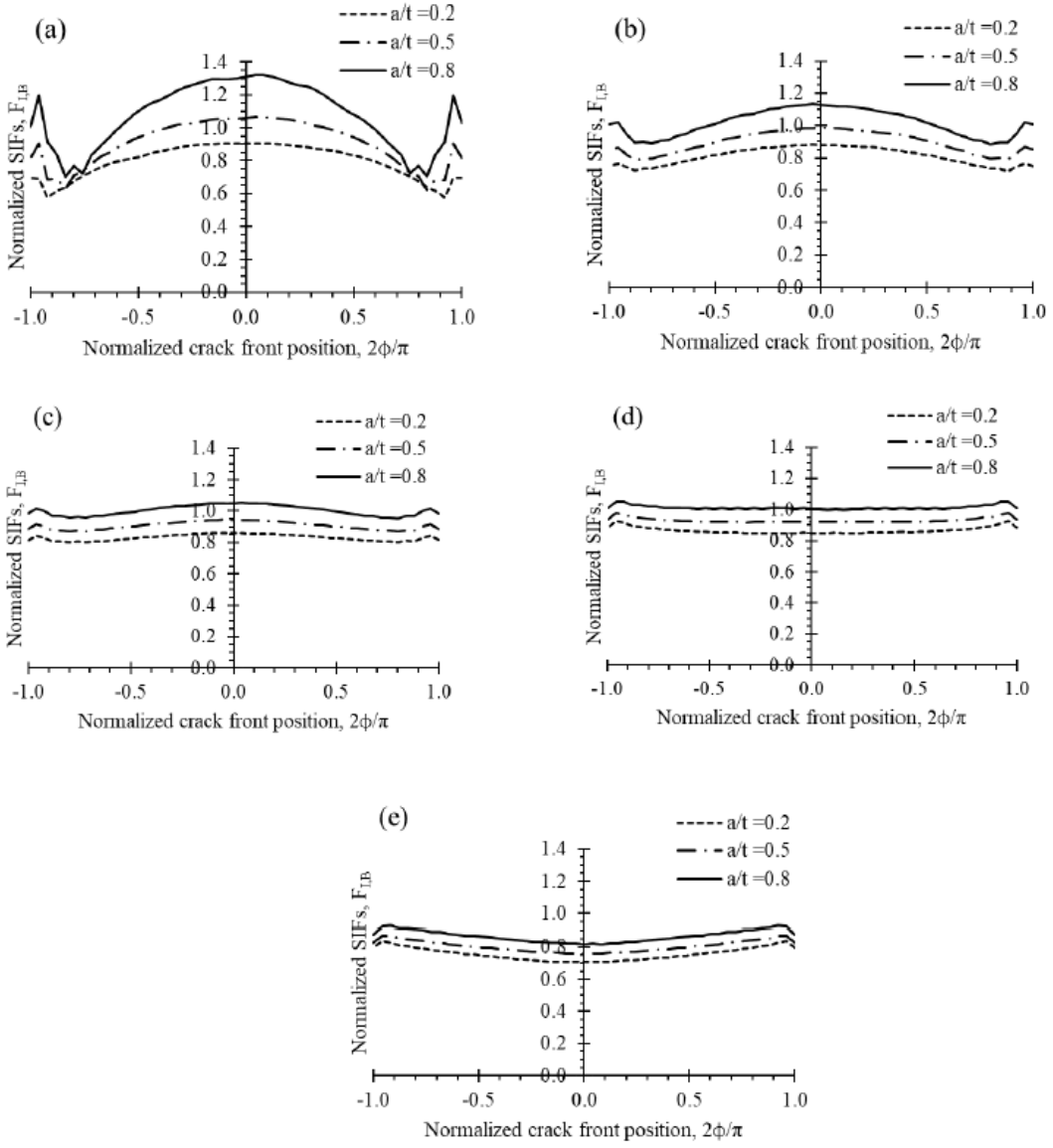

Fig. 8 - Distribution of mode I SIFs with respect to the crack front, for an Internal crack subjected to bending, where (a) a/c=0.4, (b) a/c=0.6, (c) a/c=0.8, (d) a/c=1, and (e) a/c=1

On the other hand, at point (B), SIFs showed an opposite behavior to that exhibited at point (A), where an inverse proportionality between the aspect ratio of the crack and the SIFs. In addition, at point (B), for the relative depth of crack with values less than 0.45, no significant effect on SIFs, while, this effect is more noticeable for deep cracks.

Figure 8 presents the orientation of the SIFs along the crack front for an internal crack under bending loading. Based on the results, the behavior, for mode I was the same to that of external crack, where, a symmetric SIFs distributed along the crack front. Furthermore, the utilized shape ratio controlling the curve shape depending on the location of the maximum value of SIF. A noticeable transition effect was detected also, and generally internal crack results found to be slightly less than those of external crack. This could lead to an impression that external crack could be treated as a serious crack compared to internal crack.

In figure 9, the behavior of the SIFs coefficients at point (A) and (B) with respect to *a/c*, is shown for an internal surface crack exposed to bending loading. The internal crack showed a typical behavior to that of external crack, except at point (A), deep cracks, *a/t*=0.8, presented convergence values of mode I SIFs, while this effect noticed on *a/t*=0.2 at point (B).

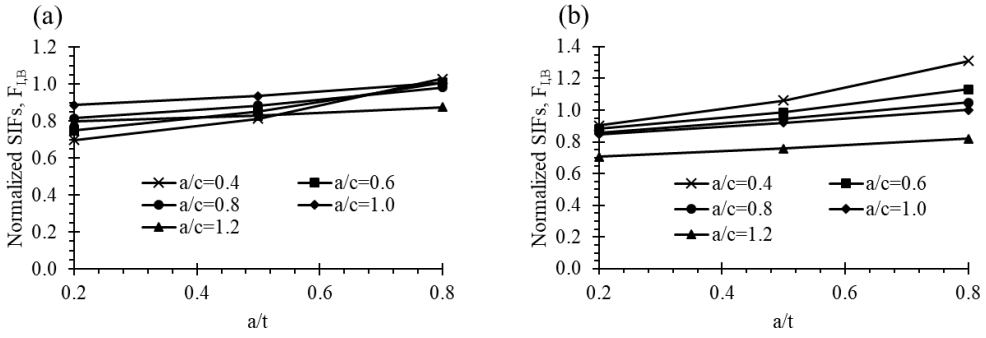

Fig. 9 - The disposal of SIFs against the relative depth of crack exposed to bending at (a) surface point (A), (b) deepest point (B) on the front of an internal crack

4.3 SIFs coefficients under torsion loading

In this section, external and internal crack analyzed under unadulterated remote torsion. For this type of loading, mode I SIFs is zero, therefore, only mode II and mode III is presented for different values of crack aspect ratio and relative depth of crack.

Figure 10 exhibits the orientation of mode II SIFs, $F_{II,T}$, for an external crack along the crack front, where it behaved in a symmetric manner. It is noteworthy that the negative value of $F_{II,T}$, denoting to the closing of the crack. In addition, *a/c*, exhibited direct proportion with $F_{II,T}$, where any rise in *a/c*, produces an increment in $F_{II,T}$, and vice versa, this is valid for cracks with $a/c \leq 1$, while higher values of aspect ratio, granting a noticeable reduction in SIFs values. All the three values of *a/t* presented an approximate similar result, which can lead to a conclusion, there is no significant effect for the relative crack depth on mode II SIFs under torsion loading. Figure 10- (f) reveals the disposal of the $F_{II,T}$ at point (A) for different values of aspect ratios, where an emphasis on the insignificant effect of *a/t* is shown.

Figure 11 showing the trend of mode III SIFs, $F_{III,T}$, for an external crack subjected to torsion loading. Again, insignificant effect for *a/t* is noticed along with an inverse proportion between *a/c*, and $F_{III,T}$. It is noteworthy for all examined crack aspect ratios, the location of the maximum $F_{III,T}$ attained on the deepest point (B) of the crack front. Figure 11-(f) showing the behavior of $F_{III,T}$ at point (B), the highest value of $F_{III,T}$ attained for *a/c*=0.4, while the minimum approached at *a/c*=1.2, in addition, the trivial impact for *a/t* for all the considered aspect ratios.

Figure 12 describes the trend of the mode II SIFs, $F_{II,T}$, for an internal crack exposed to torsion loading. Again, the internal crack showed a typical behavior to that of external crack, where, insignificant effect for *a/t* on $F_{II,T}$ distribution. Whereas, the $F_{II,T}$ behavior at the point (A) for internal crack, figure 12-(f), was the inverse to what has been seen for the external crack. Where, higher values of *a/c*, gave the highest value of $F_{II,T}$, this also valid for $a/c \leq 1$, but for higher values of aspect ratio, $F_{II,T}$ comes with a reduction in its values.

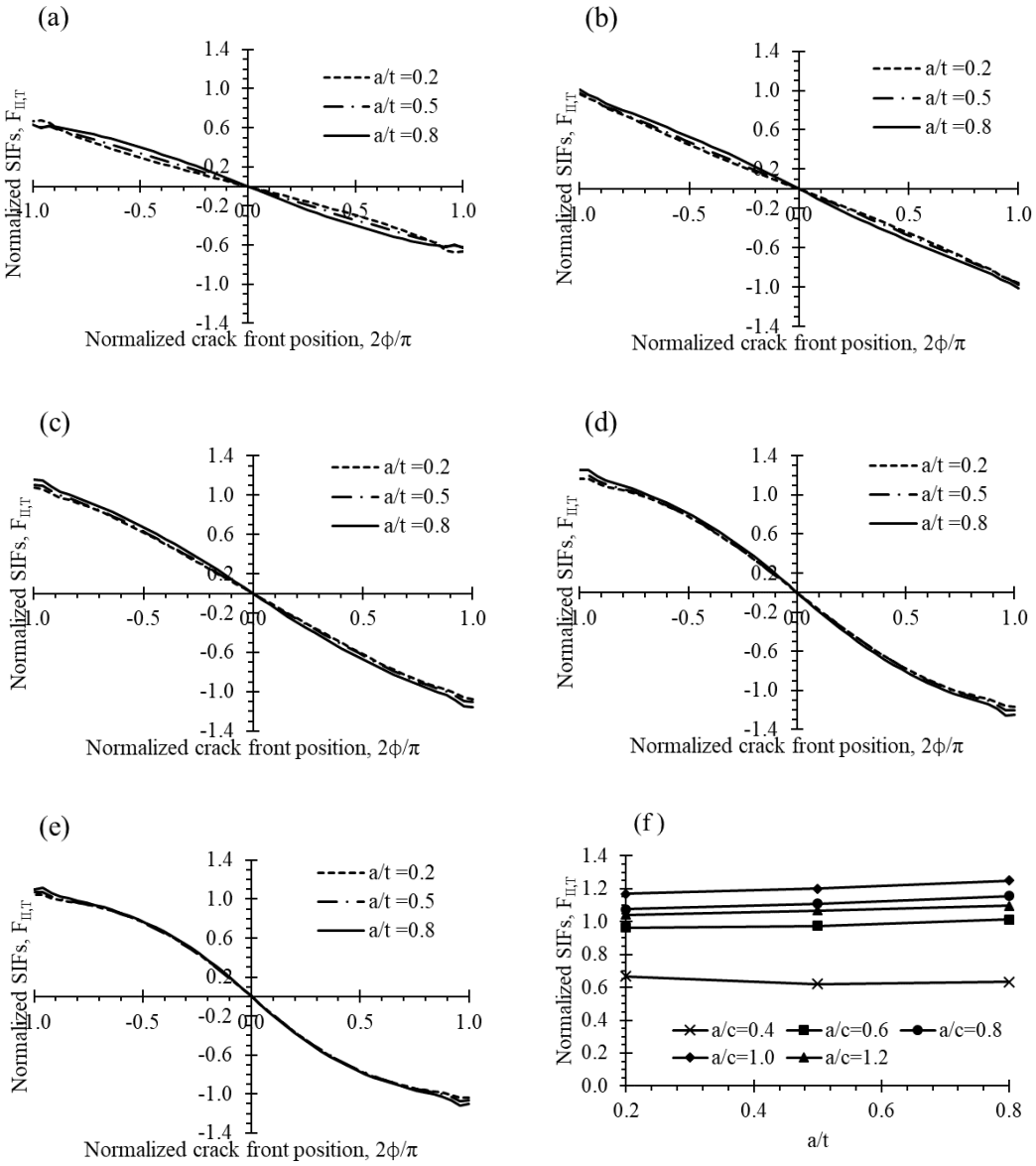

Fig. 10- Distribution of mode II SIFs along crack front for an external crack under torsion, where (a) a/c=0.4, (b) a/c=0.6, (c) a/c=0.8, (d) a/c=1, (e) a/c=1.2 and (f) SIFs behavior at surface point

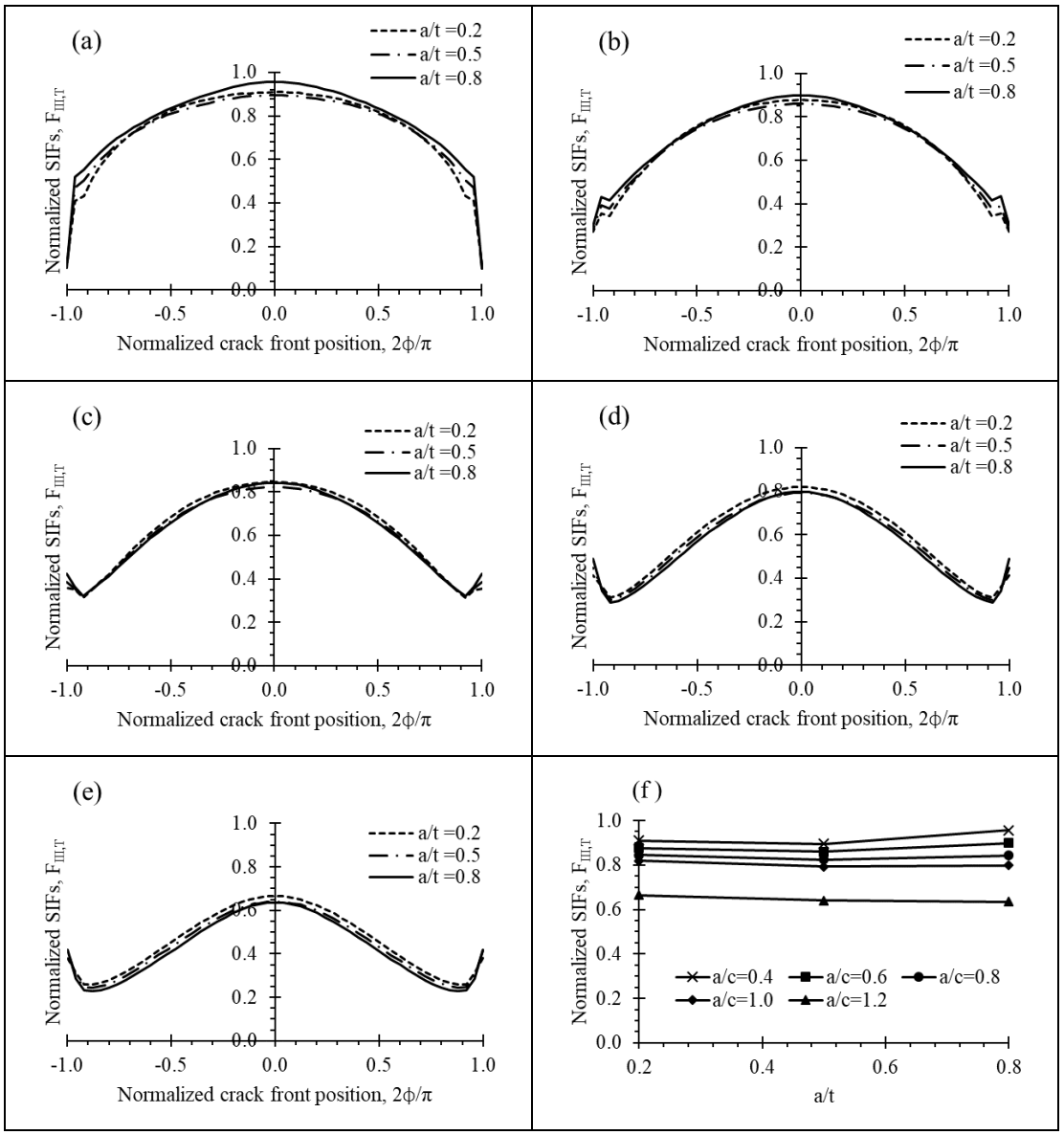

Fig. 11 - Trend of mode III SIFs of un external surface crack under torsion loading, where (a) a/c=0.4, (b) a/c=0.6, (c) a/c=0.8, (d) a/c=1, (e) a/c=1.2 and (f) SIFs behavior at deepest point

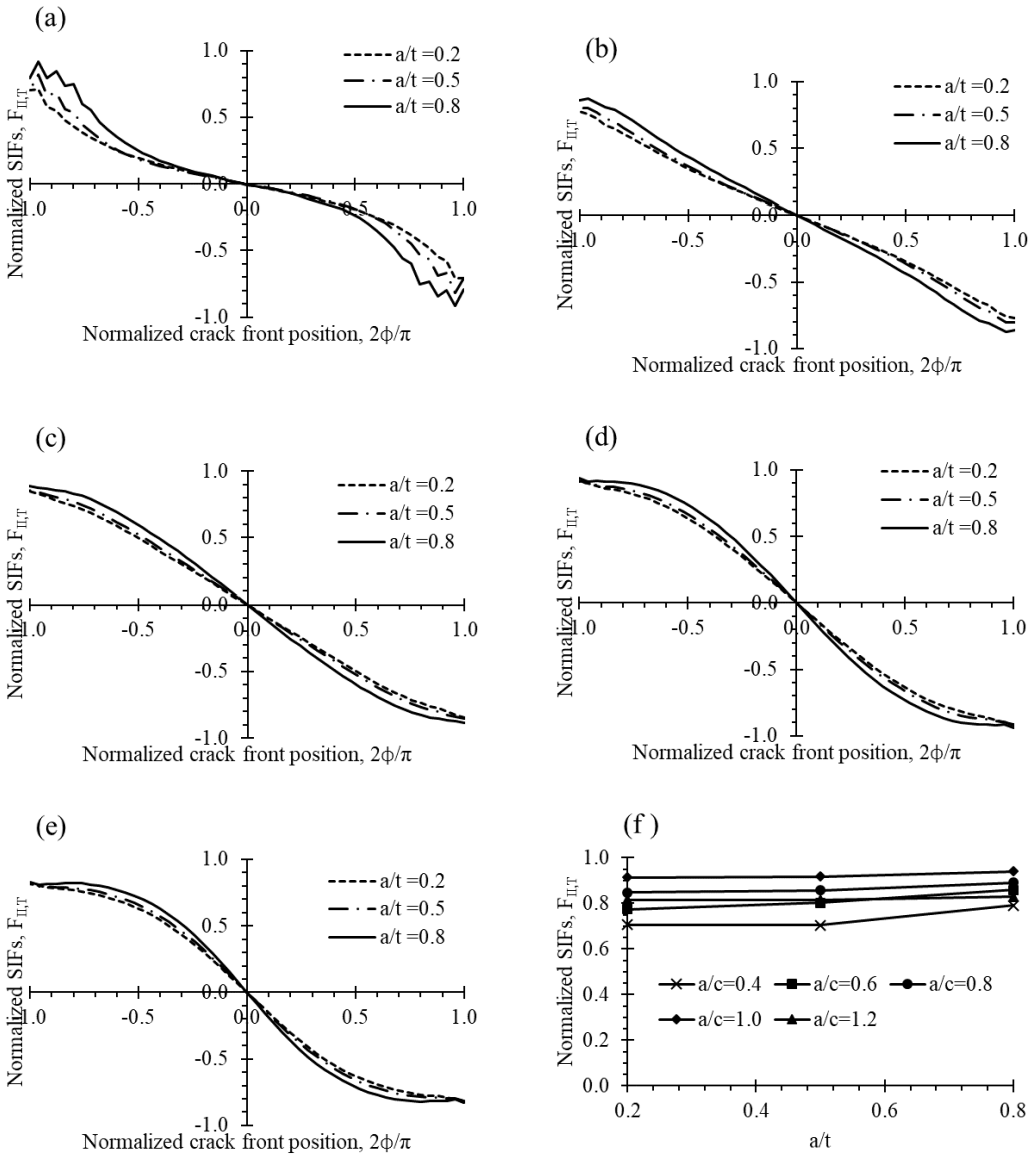

Fig. 12 - Orientation of mode II SIFs along crack front for an internal crack under torsion, where (a) a/c=0.4, (b) a/c=0.6, (c) a/c=0.8, (d) a/c=1, (e) a/c=1.2 and (f) SIFs behavior at surface point

Figure 13 depicts the dissemination of the normalized mode III SIFs influence coefficients $F_{III,T}$, for an inner surface crack exposed to remote torsion load. Remarkable behavior found for the internal crack, where for mode III, the crack showed resistance against crack propagation, which was not seen for the external crack. Furthermore, under torsion loading, an internally cracked cylinder will never fail with mode III type of failure because of the resistance of crack faces to the crack propagation. The position where the maximum value of $F_{III,T}$ on the crack front is attained always laying on the deepest point (B). In term of value, an obvious inversely proportion relationship can be seen between crack aspect ratio and the maximum value of $F_{III,T}$, where the highest value achieved at a/c=0.4, while gradually the value of $F_{III,T}$ decreasing with the increase of the aspect ratio. The relative depth of the crack showed significant effect especially for $a/c \leq 1$, figure 13- (f).

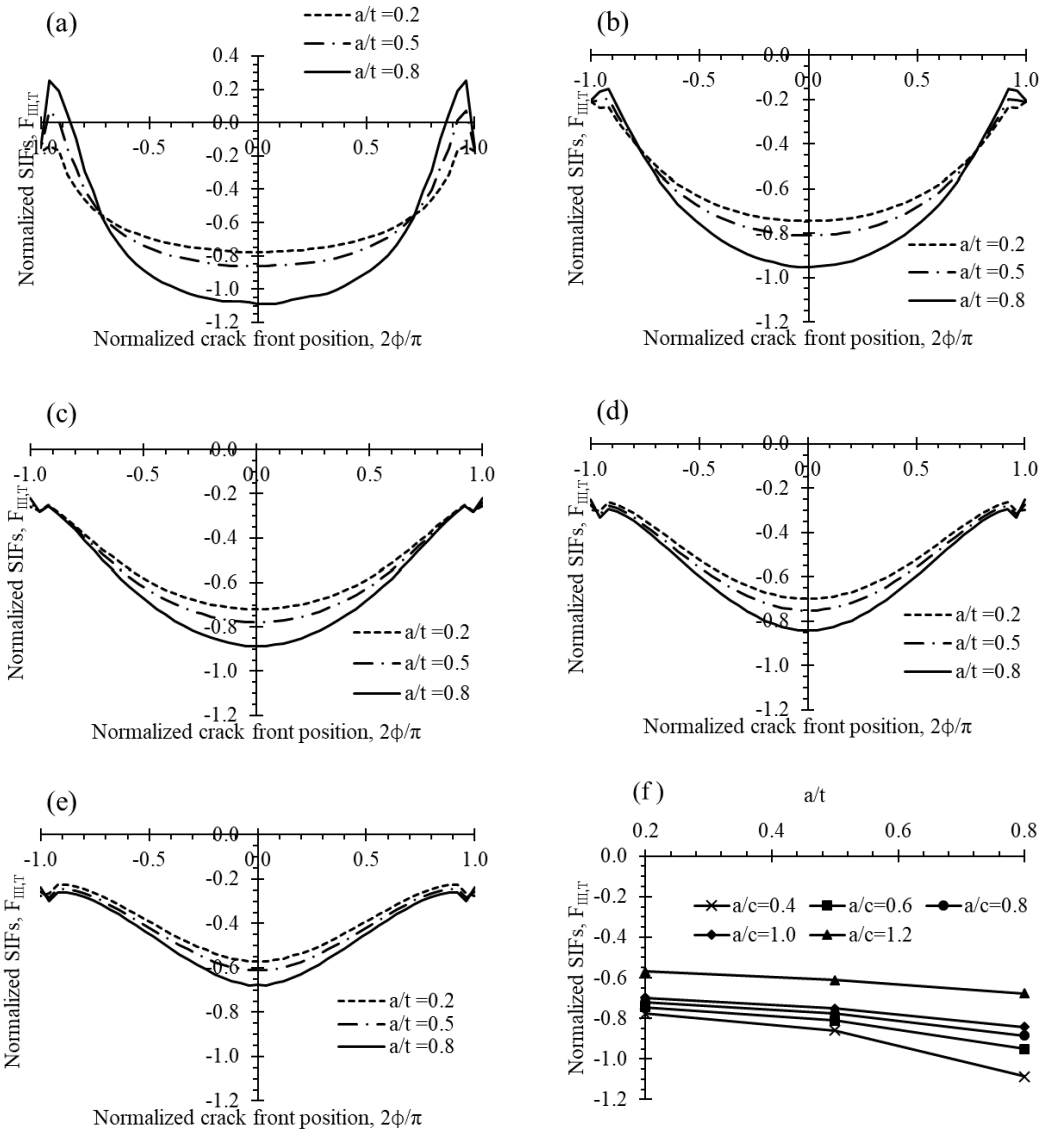

Fig. 13 - Trend of mode III SIFs for an internal surface crack under torsion loading, where (a) a/c=0.4, (b) a/c=0.6, (c) a/c=0.8, (d) a/c=1, (e) a/c=1.2 and (f) SIFs behavior at deepest point

5. Conclusion

In this paper, a thick cylinder with an internal and external surface crack examined under the effect of remote bending and torsion loading conditions. A linear elastic fracture mechanics parameter, stress intensity factor (SIFs) was calculated along the crack front for each considered crack configurations. The shape ratio of the crack or crack aspect ratio, *a/c*, assumed to change from 0.4 to 1.2, and for each value of shape ratio, three values of depth ratio, *a/t*, vary between 0.2, 0.5 and 0.8. For all the considered cases in this study, R_i/R_o =0.8, and R_i/t =4. Under bending loading condition only mode I SIFs presented, while mode II and III presented for torsional loading. Based on finding for both external and internal cracks under bending loading, SIFs distributed symmetrically along the crack front and the point where the maximum value of SIFs attained laying either at the surface point or at the deepest point of the crack front. The location where maximum SIFs approached, strongly depend on the crack aspect ratio, therefore, a transition effect noticed. The behavior of SIFs at the surface and deepest point with respect to crack aspect ratio is the opposite. Whereas for torsion loading, the orientation of mode II and mode III SIFs found to be symmetric along the crack front for both external and internal cracks. Mode II for both cracks approximately is similar, indicating to the insignificant effect for the relative depth of the crack. A remarkable behavior can be deduced from mode III for both cracks, where the external crack showed an opposite trend manner to that of internal, which means an internally cracked cylinder will never fail under mode III of failure, due to the resistance of the crack to propagates. Finally, for torsion loading, the effect of relative crack depth is slightly higher than those of bending moment.

References

[1] X. B. Lin and R. A. Smith, "Fatigue growth prediction of internal surface cracks in pressure vessels," *J. Press. Vessel Technol.*, vol. 120, no. 1, pp. 17–23, 1998.

[2] G. de C. Coêlho, A. A. Silva, M. A. Santos, A. G. B. Lima, and N. C. Santos, "Stress Intensity Factor of Semielliptical Surface Crack in Internally Pressurized Hollow Cylinder—A Comparison between BS 7910 and API 579/ASME FFS-1 Solutions," *Materials (Basel).*, vol. 12, no. 7, p. 1042, 2019.

[3] J. Underwood, "Stress Intensity Factors for Internally Pressurized Thick-Wall Cylinders," in *Stress Analysis and Growth of Cracks: Proceedings of the 1971 National Symposium on Fracture Mechanics: Part 1*, 100 Barr Harbor Drive, PO Box C700, West Conshohocken, PA 19428-2959: ASTM International, 1972, pp. 59-59–12.

[4] K. Miyazaki and M. Mochizuki, "The effects of residual stress distribution and component geometry on the stress intensity factor of surface cracks," *J. Press. Vessel Technol.*, vol. 133, no. 1, p. 11701, 2011.

[5] A. E. Ismail, M. K. Awang, A. L. Mohd Tobi, and M. H. Ahmad, "Mode I stress intensity factors of slanted cracks," *ARPN J. Eng. Appl. Sci.*, vol. 12, no. 10, pp. 3189–3194, 2017.

[6] A. E. Ismail *et al.*, "Combined mode I stress intensity factors of slanted cracks," in *IOP Conference Series: Materials Science and Engineering*, 2017, vol. 226, no. 1, p. 12011.

[7] I. S. Raju and J. C. Newman, "Stress-intensity factors for circumferential surface cracks in pipes and rods under tension and bending loads," in *Fracture mechanics: seventeenth volume*, ASTM International, 1986.

[8] A. E. Ismail, A. K. Ariffin, S. Abdullah, and M. J. Ghazali, "Stress intensity factors under combined tension and torsion loadings," Indian Journal of Engineering and Materials Science, vol. 19, pp. 5-16, 2012.

[9] A. E. Ismail, A. K. Ariffin, S. Abdullah, M. J. Ghazali, M. Abdulrazzaq, and R. Daud, "Stress intensity factors under combined bending and torsion moments," *J. Zhejiang Univ. Sci. A*, vol. 13, no. 1, pp. 1–8, 2012.

[10] A. E. Ismail, A. K. Ariffin, S. Abdullah, and M. J. Ghazali, "Stress intensity factors for surface cracks in round bar under single and combined loadings," *Meccanica*, vol. 47, no. 5, pp. 1141–1156, 2012.

[11] I. S. Raju and J. C. Newman, "Stress-Intensity Factors for Internal and External Surface Cracks in Cylindrical Vessels," *J. Press. Vessel Technol.*, vol. 104, no. 4, pp. 293–298, Nov. 1982.

[12] A. Carpinteri, R. Brighenti, and A. Spagnoli, "Fatigue growth simulation of part-through flaws in thick-walled pipes under rotary bending," *Int. J. Fatigue*, vol. 22, no. 1, pp. 1–9, 2000.

[13] A. Carpinteri and R. Brighenti, "Circumferential surface flaws in pipes under cyclic axial loading," *Eng. Fract. Mech.*, vol. 60, no. 4, pp. 383–396, 1998.

[14] C.-Q. Li and S. T. Yang, "Stress intensity factors for high aspect ratio semi-elliptical internal surface cracks in pipes," *Int. J. Press. Vessel. Pip.*, vol. 96, pp. 13–23, 2012.

[15] S. T. Yang, Y. L. Ni, and C.-Q. Li, "Weight function method to determine stress intensity factor for semi-elliptical crack with high aspect ratio in cylindrical vessels," *Eng. Fract. Mech.*, vol. 109, pp. 138–149, 2013.

[16] A. Zareei and S. M. Nabavi, "Calculation of stress intensity factors for circumferential semi-elliptical cracks with high aspect ratio in pipes," *Int. J. Press. Vessel. Pip.*, vol. 146, pp. 32–38, 2016.

[17] J. Predan, V. Močilnik, and N. Gubeljak, "Stress intensity factors for circumferential semi-elliptical surface cracks in a hollow cylinder subjected to pure torsion," *Eng. Fract. Mech.*, vol. 105, pp. 152–168, 2013.

[18] A. R. Shahani and S. E. Habibi, "Stress intensity factors in a hollow cylinder containing a circumferential semi- elliptical crack subjected to combined loading," *Int. J. Fatigue*, vol. 29, no. 1, pp. 128–140, 2007.

[19] O. M. Al-Moayed, A. K. Kareem, A. E. Ismail, S. Jamian, and M. N. Nemah, "Distribution of Mode I Stress Intensity Factors for Single Circumferential Semi-Elliptical Crack in Thick Cylinder," *Int. J. Integr. Eng.*, vol. 11, no. 7, pp. 102–111, 2019.

[20] M. N. Fakhri, O M; Kareem, A K; Ismail, A E; Jamian, S; Nemah, "Mode I SIFs for internal and external surface semi-elliptical crack located on a thin cylinder," *TEST Eng. Manag.*, vol. 81, no. 77777, pp. 586–596, 2019.

[21] "No Title," 2016.

[22] A. E. Ismail, "Mode I stress intensity factors of sickle-shaped surface cracks in round solid bars under bending moment.," *Int. J. Automot. Mech. Eng.*, vol. 13, no. 2, pp. 3329–3344, 2016.

[23] A. Fahem, A. Kidane, and M. A. Sutton, "Geometry factors for Mode I stress intensity factor of a cylindrical specimen with spiral crack subjected to torsion," *Eng. Fract. Mech.*, vol. 214, pp. 79–94, 2019.